MAUSAM, **75**, 2 (April 2024), 461-478

MAUSAM

DOI : https://doi.org/10.54302/mausam.v75i2.6058
Homepage: https://mausamjournal.imd.gov.in/index.php/MAUSAM

UDC No. 551.577.61 (541.35)

Rainfall threshold for landslide awareness – Focusing on the case study in the landslide EVO pilot area region in western Nepal

JAGAT K BHUSAL, JANAK L. NAYAVA, SARAJU K. BAIDYA*, BIKASH NEPAL**,
WOUTER BUYTAERT*** and BHANU NEUPANE*#

CoI, Landslide EVO

**Secretary, GoN*

***Meteorologist, DHM*

****Professor, Imperial college*

*#*UNESCO*

(*Received 3 November 2022, Accepted 03 August 2023*)

e mail : bhusaljagat@gmail.com

सार – नेपाल की ऊबड़-खाबड़ स्थलाकृति, अस्थिर नई भौगोलिक संरचनाएं और भंगुर चट्टानें देश को भूस्खलन, मृदा अपरदन और मलबा गिरने जैसे जल-प्रेरित खतरों के प्रति अत्यधिक संवेदनशील बनाती हैं। भारी वर्षा के दौरान पहाड़ी जलक्षेत्र और पहाड़ियों तथा नदी तटों की बस्तियाँ प्राकृतिक रूप से असुरक्षित हो जाती हैं। भूस्खलन ईवीओ परियोजना के लिए दो भूस्खलन क्षेत्रों का यथा - बाजुरा जिले में बाजेडी भूस्खलन, और दूसरा नेपाल के बझांग जिले में सनकुडा भूस्खलन का चयन कियागया । स्वचालित वर्षामापी स्थापित किए गए, और 2019 और 2021 के लिए डेटा दर्ज किया गया। सबसे उपयुक्त प्रवृत्ति रेखाएं विभिन्न अवधियों की प्रेक्षित वर्षा की अधिकता से निर्धारित होती हैं। इसके अलावा, वर्ष 2019 में पायलट क्षेत्रों के बाहर के क्षेत्र में हुई 24 घंटे की वर्षा के रिकॉर्ड और भूस्खलन की घटनाओं का भी विश्लेषण और सहसंबद्ध किया गया। वर्षा की तीव्रता और गंभीरता विभिन्न अवधियों के लिए अधिकतम, न्यूनतम और औसत गंभीरता के अनुरूप सहसंबद्ध होती है। वर्षा की गंभीरता और अवधि के आंकड़ों के बीच सहसंबंध में एक उत्कृष्ट समुच्चय देखा गया। क्षेत्र के भूस्खलन जोखिम मूल्यांकन के लिए ट्रेंडलाइन को वर्षा प्रभाव सीमा माना जाता है।

ABSTRACT. Nepal's rugged topography, unstable young geological formations, and fragile rocks make the country highly vulnerable to water-induced hazards such as landslides, soil erosion, and debris torrents. Hilly watersheds and settlements in hills and river banks are naturally vulnerable during heavy rainfall. The landslide EVO project selected two landslide areas, one the Bajedi landslides in the Bajura district, and another Sunkuda landslides in Bajhang district of Nepal. Automatic rain gauges were installed, and data were recorded for 2019 and 2021. The best-fit trend lines are determined by the observed rainfall depths of different durations. In addition, 24-hour rainfall records and landslide events that occurred in the region outside the pilot areas in the year 2019 were also analyzed and correlated. Rainfall intensities and depths corresponding to maximum, minimum, and average depth are correlated for different durations. The correlation between rainfall depths and durations data showed an excellent fitting observed. The trend line is considered as the rainfall threshold line for landslide risk assessment for the region.

Key words – Rainfall depth, Depth ratio, Landslide, EVO-project.

1. Introduction

In the world, Nepal is the 20th most affected country due to multi-hazards (UN. Office for Disaster Risk Reduction, 2020). Over a north-south distance of about 200 km, elevation ranges from 70 m to 8848 m in Nepal. This spatial variation, together with highly rugged topography, unstable geological structures, and fragile rocks, makes the country highly vulnerable to water-induced hazards such as landslides, soil erosion, floods, and debris torrents (Dahal, 2012). Inherent natural factors include geological formation and structure, slope, aspect,

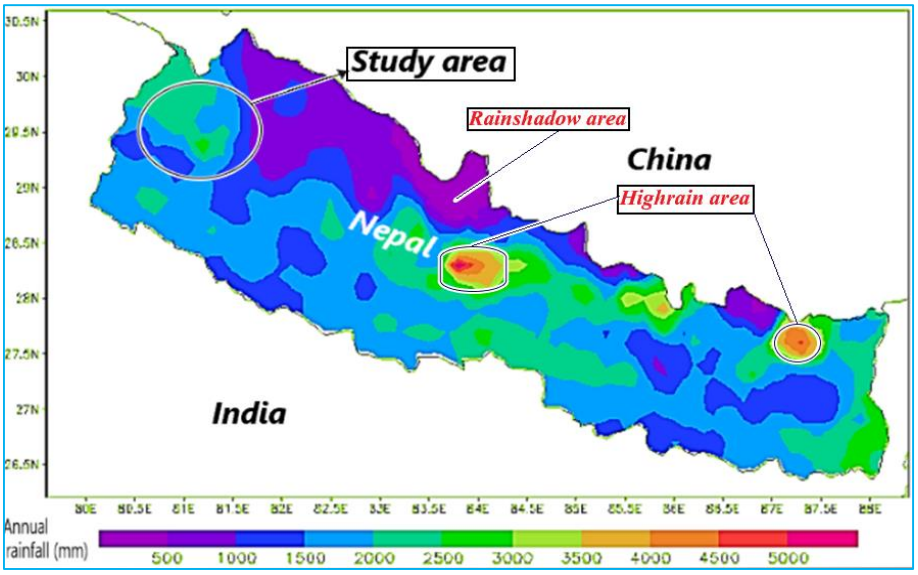

Fig. 1. Spatial distribution of annual rainfall in Nepal (MOSTE, 2014).

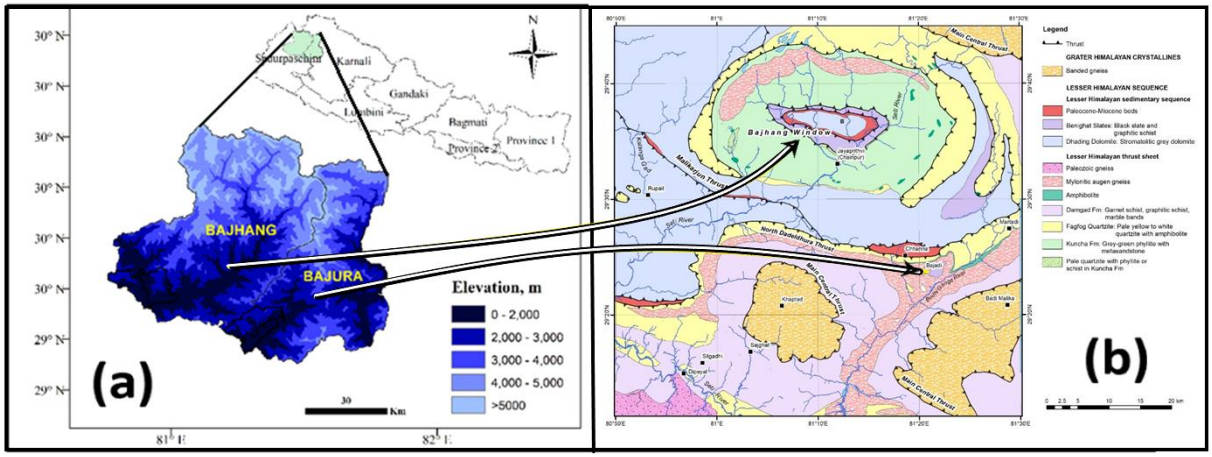

Figs. 2(a&b). Pilot area location in Bajhang-Bajura [*Source*-Elevation map (a) from Nayava *et al*., 2022; and map (b) showing main geological structures from Dhital, 2022]

land use, ground cover and ground conditions; and external factors are earthquakes and rainfall duration/intensity. Generally, the causes of landslides occurring are either natural or human-induced and their likeliness is enhanced when two factors combine. Anthropogenic factors include human interventions such as deforestation, improper land use, unplanned construction, and unplanned mining. The weak geotectonic characteristics of the Himalayas make it vulnerable to heavy rainfall and earthquakes. Rainfall and earthquakes are also triggering agents of landslides. The topographical feature and geological nature of mountains in combination with the duration and intensity of rainfall are directly related to the probability of landslides and extreme debris torrents in Nepal (Bhusal, 1994). Landslides occur mostly during the monsoon season. It is also said that, Nepal is at a new crossroads with new opportunities to rein in dozer road constructors, but this will require concerted effort and considerably more political willpower than has been demonstrated over the last decade (Sudmeier-Rieux, *et al*., 29 March, 2019).

The annual normal precipitation in Nepal is below 1000 mm in the higher mountain region with the Mustang receiving the lowest annual precipitation (<500 mm). The highest annual precipitation (>5000 mm) is observed in the Kaski district of Gandaki province along with two other precipitation pockets in the Sindhupalchowk (Gumthang) and Sankhuwasabha (Num) districts with >4000 mm annual precipitation. Except in the high-Himalayan region, annual rainfall over large parts of the remaining areas of the country is greater than 1500 mm (Fig. 1). The elevation and main geological feature of the study region is shown in Figs. 2 (a&b).

Except in some rain shadow areas behind the Himalayas (Fig. 1) and two areas of the high rainfall pocket, the spatial and quantitative distribution of annual rainfall in the study area (pilot region) falls broadly under a similar pattern that occurs in most mountain regions of Nepal.

2. The study area

In this study, far western mountainous region of Nepal was chosen to focusto two landslide areas. [Figs. 2(a&b)]. Pilot areas are characterized by extremely rugged topography in the Lesser Himalayan Sequence (Cieslik *et al*., 2019), with an elevation ranging from 720 to 6960 m. The Bajedi landslides in the Bajura district and the Sunkuda landslides in the Bajhang district are two pilot areas. Both locations experience seasonal shallow slides (<1 m depth): rockslides in Bajedi and soil slides in Sunkuda.

The Bajedi landslide lies near the north end of the Dadeldhura thrust sheet, which is part of the Lesser Himalayan nappe. The total area in Bajedi landslides was found to be affected by deep-seated gravitational slope deformation (DSGSD) of approximately 29.8 km^2 at elevations between 950 m and 2150 m above mean sea level (amsl). It stretches between Dadeldhura, Dipayal, Sanphe Bagar, and Martadi. It is about 100 km long and 20 km wide. The Lesser Himalayan nappe forms a syn form and rests over grey stromatolitic dolomite and black slates. The bedrock is characterized by a series of overlapping quartzites and phyllites. DSGSD generates loose material and debris flow with potentially severe consequences for communities in the lower Budhi Ganga river valley. Although quartzites is mechanically strong and impermeable, they are nonetheless slowly affected by rainfall penetration. The pilot areas lie in a relatively high density of east-west trending thrust faults, allowing a greater degree of percolation (Parajuli *et al*., 2020; Paul *et al*., 2020).

2.1. *Data-rainfall and landslide events*

2.1.1. *Rainfall data*

The Olena rainfall station is located near Bajedi landslides in the Bajura district at 1116 m in the very narrow valley of the Budhi Ganga River, generally oriented east to west. The Rainfall Station in Sunkuda is near the Sukunda landslides in Bajhang district and is located 894 m above the mean level. Furthermore, long-term rainfall data from 17 locations were analyzed to study the general pattern of rainfall on a broader scale. The Landslides EVO of Western Nepal under Imperial College has installed 13 rainfall stations at 10 locations

Fig. 3. Location of Bajedi landslide & AWS stations

Fig. 4. Location of Sunkuda landslide & AWS stations

Fig. 5. Selected networks surrounding the pilot areas. (*Source* DHM)

around the Bajedi landslide (Fig. 3) and two rainfall stations around the study of Sukunda landslides (Fig. 4). The Bajedi landslide, located in the Budhi Ganga Municipality, is a large chronic landslide with an area of 0.55 square kilometers and a perimeter of 5.2 kilometers. The precipitation over and around landslide areas was monitored using rain gauges which have recorded rainfall events from May to September 2021. Extreme rainfall data from 21 stations operated by the Department of Hydrology and Meteorology (DHM) of the region along with monsoon rainfalls recorded by 10 automatic tipping

TABLE 1

Rainfall stations under DHM and automatic rain gauges at Landslides EVO sites

Stn ID	Place	Latitude	Longitude	District
Location of rainfall station-DHM Networks				
101	Kakerpakha	29.65	80.5	Baitadi
102	Gothalapani	29.5574	80.4132	Baitadi
103	Patan	29.4671	80.5458	Baitadi
104	Dadheldura	29.3014	80.5878	Dadheldura
108	Satbanjh	29.4973	80.4974	Baitadi
201	Pipalkot	29.6188	80.8479	Bajhang
202	Chainpur	29.55	81.2167	Bajhang
203	Silgadi	29,268	80.9836	Doti
204	Bajura	29.3833	81.3167	Bajura
205	Katai	29	81.1333	Doti
206	AsaraGhat	28.9503	81.4443	Achham
107	Darchula	29.85	80.5667	Darchula
210	BanggaCamp	28.9646	81.1498	Achham
214	KolaGaun	29.1202	80.7094	Doti
218	Dipayal	29.2621	80.9369	Doti
302	Thirpu	29.3032	81.7519	Kalikot
305	SeriGhat	29.13	81.5884	Kalikot
308	Nagma	29.2006	81.9106	Kalikot
309	Bijayapur	29.2495	81.6391	Kalikot
224	Olena	29.23	81.19	Bajura
225	Sukunda	29.49	80.90	Bajhang
Location of rainfall station- LEVO Networks				
RG1	Sunkuda Sec. School	29.504	80.851	
RG2	Upper Bajedi School	29.3916	81.3468	
RG3	Lower Bajedi School	29.3782	81.3486	
RG11	Thuma School	29.3761	81.3317	
RG13	Nearby mill, Chededaha	29.4039	81.3208	
RG14	Asha Hotel	29.382	81.3664	
RG15	Nearby mill, Chededaha	29.4039	81.3208	
RG16	Near lake	29.4172	81.3122	
RG17	JB Malla House, Sunkuda	29.5036	80.8722	
RG18	SB Kathayat's House	29.417	81.3312	
RG19	DHM Station, Olena	29.23	81.19	

bucket-type rainfall stations of the year 2019 and 2021 are considered in knowledge generation (Fig. 5 & Table 1).

2.1.2. *Observed rainfall intensities (2019 & 2021) at different durations.*

Data from automatic rainfall stations were collected, screened, and rainfall depths were extracted at different durations from 15 minutes to 72 hours for each network station (Table 2).

2.1.3. *Landslide events and the corresponding day rainfall in 2019.*

There are thirty-seven stations in the region. Out of 37 locations, 11 locations had received the maximum downpour between 24.6 mm and 126 mm on day 1, six locations received the maximum downpour between 20 mm and 81 mm on day 2, seven locations received the maximum downpour between 27 mm and 111 mm on day 3, five locations received the maximum downpour between 25 mm and 43 mm on day 4, four locations received the maximum downpour between 17 mm and 22 mm on day 5 and one location received rain continuously for more than five days (Table 3).

The maximum 1-day rainfall in 2019 over project areas was 126 mm (24 July). 111 mm (13 September) and 81 mm (9 July).

Landslides were reported during all of those rainy days (Table 3), which are broadly grouped as follows:

(*i*) Landslides which occurred from 8 July to 12 July should be taken into account by the rainfall depths of 71.6 mm (8 July), 81.3 mm (9 July), 43,6 mm, (10, 11/ 12 July) and 22.7 mm (12 July).

(*ii*) Landslides that occurred from 13 July to 16 July should be taken into account by 72 mm (13 July), 30 mm (14 July), 61 mm (15 July) and 41 mm (16 July).

(*iii*) Landslides that occurred from 24 July to 26 July should be taken into account by 38.2 mm (24 July), 126.2 mm (25 July) and 33.2 mm (26 July).

(*iv*) Landslides that occurred from 31 July to 1 August should be taken into account by 38.9 mm (31 July), 33 mm (1 August).

(*v*) Landslides that occurred from 24 July to 26 July should be taken into account as 38 mm (24 July), 126.2 mm (25 July), 40 mm (25 July) and 33 mm (26 July).

(*vi*) Landslides that occurred from 5 August to 6 August should be taken into account by 80.3 mm (6 August).

(*vii*) Landslides that occurred from 21 August to 24 August should be taken into account by 35 mm (21 August).

TABLE 2

Rainfall depths at different durations in observation data

2019 data of LEVO sites	Rainfall in mm at different duration										
Location	Ele m	15 min	30 min	1 hour	2 hour	3 hour	6 hour	12 hour	24 hours	48 hours	72 hours
Asha Hotel-19	1020	11.2	13.6	14	17	20	48	64	90	91.2	150.8
Bajedi lower School-19	1162	12	14	15	33	40	42	79	101	102.4	161.6
Bajedi upper School-19	1624	12.8	18	21.6	33	37	44	76	108.4	118.6	123.2
Kathayat house-19	1860	15.6	29.6	32	53	57	68	113	130.2	133.6	159.2
Water mill Cheda-19	2030	19	36.8	47	79	86	96	127	147	150.8	186
Near Lake, Cheda-19	2040	17.6	21.8	26	50	59	81	109	124	128.6	149.6
2021 data of LEVO sites											
Asha Hotel-2021	1020	17	28.6	35	49.4	50.4	51.8	57.8	86.6	101.6	111.6
Retired Sir-2021	1274	12.4	19.8	27.8	38.2	38.6	60.2	103.2	191.4	307.6	316.4
Thuma Sec. School-2021	1447	17	26.6	35.8	54.2	64.8	67.2	69.4	75.2	101.4	111.2
Sunkunda School-2021	1594	21.2	25.6	45	45.2	45.4	56.6	99.2	187.8	301.4	312
Kathayat House 2021	1860	17	28.4	42.8	58.4	70.2	75	79.6	136.2	214.2	225.2
Maximum (mm)		21.2	36.8	47	79	86	96	127	191.4	307.6	316.4
Minimum (mm)		11.2	13.6	14	17	20	42	57.8	75.2	91.2	111.2
Average (mm)		15.709	23.891	31.091	46.4	51.673	62.709	88.836	125.25	159.22	182.44

(*viii*) Landslides that occurred from 5 August to 6 August should be taken into account by 80.3 mm (6 August).

(*ix*) Landslides that occurred from 31 August to 1 September should be taken into account by 48 mm (30 August) and 86.8 mm 1 September).

(*x*) Landslides that occurred from 12-14 September should be taken into account by 24.4 mm (12 September). 111.8 mm (13 September) and 27.5 mm (14 September).

(*xi*) Landslides that occurred from 23-24 September should be taken into account by 64.4 mm (24 September). 33 mm (25 September).

(*xii*) Landslides occurred from 27-30 September should be taken into account by 35.4 mm (30 September).

2.2. *Methodology*

Quartile analysis describes the variation and distribution of data within the time period considered for the analysis. The plot shows the maximum, minimum, and three quartiles (25, 50 and 75 percentiles). This method helps to find outliers. The arithmetic mean or median has its own advantages and disadvantages. The median was preferred over the mean, as the former is not influenced by the exceptional AMS (annual maximum series) values.

Rainfall intensities of 15 minutes, 30 minutes, 45 minutes, 1-h, 2-h, 3-h, 6-h, 12-h, 48-h and 72-h were determined by the location of automatic stations established by the landslide EVO research projects. Similarly, the intensities of the 24-hour rainfall (daily rainfall), 48-hour and 72-hour durations were determined from the annual maximum rainfall series of the manual stations received from the DHM data bank.

A trend line, also referred to as a line of best fit, is a straight or curved line in a chart that shows the general pattern or overall direction of the data. This analytical tool is most often used to show data movements over a period of time or correlation between two variables. (https://www.youtube.com/watch?v=0ienbLvFddQ. Retrieved on 1 July, 2022).

The exact timing of the landslide and the corresponding rainfall intensities in and around the areas are useful for understanding and relating. But there were no such events recorded in the study region. Therefore, days when landslides occurred in 2019 were collected and corresponding 1-day, 2-day, 3-day or more rainfall were

TABLE 3

Selected daily rainfall data that resulted in landslides events in respective districts

Landslide events & daily rainfall			2019		Daily rainfall in millimeter					Cumulative rainfall in mm				
S.No.	St No	Location	Day	Mon.	1 day	2 day	3 day	4 day	5 day	24 hr.	48 hr.	72 hr.	96 hr.	120 hr.
1	109	Lumpthi	30 - 31	Aug	48.0	5.5	NS	NS	NS	24 hr.	48 hr.	72 hr.	96 hr.	120 hr.
2	109	Lumpthi	21 - 24	Aug	35.0	3.0	5.0	8.5	NS	48.0	53.5	NS	NS	NS
3	231	Kalukheti	25 - 26	Aug	27.4	11.7	NS	NS	NS	35.0	38.0	43.0	51.5	NS
4	210	Banga Camp	24 -25	July	126.2	13.3	NS	NS	NS	27.4	39.1	NS	NS	NS
5	109	Lumpthi	13 - 16	July	72.0	30.0	0.0	41.0	NS	126.2	139.5	NS	NS	NS
6	107	Darchula	8 - 10	July	71.6	24.0	2.0	NS	NS	72.0	102.0	102.0	143.0	NS
7	107	Darchula	25 - 26	July	40.0	7.5	NS	NS	NS	71.6	95.6	97.6	NS	NS
8	206	AsaraGhat	24 - 25	July	38.2	6.7	NS	NS	NS	40.0	47.5	NS	NS	NS
9	201	Pipalkot	1 - 3	Sept	86.8	7.1	13.8	NS	NS	38.2	44.9	NS	NS	NS
10	309	Bijayapur (Raskot)	5 - 6	June	18.4	20.2	NS	NS	NS	86.8	93.9	107.7	NS	NS
11	107	Darchula	29 - 30	Aug	14.8	55.7	19.0	NS	NS	18.4	38.6	NS	NS	NS
12	204	Bajura (Martadi)	14 - 16	Aug	18.5	50.8	9.4	NS	NS	14.8	70.5	89.5	NS	NS
13	109	Lumpthi	8 - 10	July	8.0	81.3	43.6	NS	NS	18.5	69.3	78.7	NS	NS
14	235	Sugali	22 - 25	Sept	3.1	64.1	33.0	5.5	NS	8.0	89.3	132.9	NS	NS
15	107	Darchula	4 - 6	Aug	21.0	4.6	80.3	NS	NS	3.1	67.2	100.2	105.7	NS
16	228	KAILASMANDU	30 - 31, 1	Jul, Aug.	4.2	24.6	38.9	NS	NS	21.0	25.6	105.9	NS	NS
17	107	Darchula	14 - 16	July	23.0	13.6	61.8	NS	NS	4.2	28.8	67.7	NS	NS
18	309	Bijayapur (Raskot)	8 - 10	July	14.8	25.0	32.6	NS	NS	23.0	36.6	98.4	NS	NS
19	204	Bajura (Martadi)	30-31, 1	July. Aug	13.7	0.0	33.0	NS	NS	14.8	39.8	72.4	NS	NS
20	218	Dipayal (Doti)	11 - 13	Sept	1.2	3.6	111.8	NS	NS	13.7	13.7	46.7	NS	NS
21	203	SilgadhiDoti	11 - 14	Sept	15.3	8.3	27.5	NS	NS	1.2	4.8	116.6	NS	NS
22	228	Kailasmandu	13 - 16	Aug	5.9	12.2	18.7	32.7	NS	15.3	23.6	51.1	NS	NS
23	305	Sheri Ghat	9 - 12	July	10.4	15.0	0.0	43.4	NS	5.9	18.1	36.8	69.5	NS
24	230	Gopghat	22 - 25	July	8.3	5.2	3.1	40.2	NS	10.4	25.4	25.4	68.8	NS
25	305	Sheri Ghat	28 - 31	July	17.0	5.3	16.4	19.3	NS	8.3	13.5	16.6	56.8	NS
26	231	Kalukheti	27 - 30	Sept	21.2	8.8	21.6	25.4	NS	17.0	22.3	38.7	58.0	NS
27	329	Manma	8 - 12	July	11.5	10.9	5.0	9.7	22.7	21.2	30.0	51.6	77.0	NS
28	109	Lumpthi	19 - 23	July	6.0	5.0	4.0	0.0	20.9	11.5	22.4	27.4	37.1	59.8
29	305	Sheri Ghat	23 - 27	July	16.7	0.0	19.3	18.3	19.4	6.0	11.0	15.0	15.0	35.9
30	329	Manma	23 - 31	July	16.9	0.9	1.3	14.4	17.7	16.7	16.7	36.0	54.3	73.7
31	109	Lumpthi	3 - 6	Aug	20.0	20.0	10.0	15.0	NS	16.9	17.8	19.1	33.5	51.2
32	232	Safebagar	22 - 25	July	5.5	8.1	0.0	6.0	NS	20.0	40.0	50.0	65.0	NS
33	201	Pipalkot	28 - 30	Sept	0.5	10.8	15.6	NS	NS	5.5	13.6	13.6	19.6	NS
34	107	Darchula	3 - 5	Sept	8.0	8.5	12.0	NS	NS	0.5	11.3	26.9	NS	NS
35	214	Kola Gaun	11 - 12	July	29.9	7.2	NS	NS	NS	8.0	16.5	28.5	NS	NS
36	234	Dumrakot	12 - 13	Sept	24.4	11.3	NS	NS	NS	29.9	37.1	NS	NS	NS
37	309	Bijayapur (Raskot)	25 - 27	July	6.4	33.2	18.6	NS	NS	24.4	35.7	NS	NS	NS

picked for analysis. Similarly, extreme rainfall of different periods 5, 15, 30, 45, 60 minutes and 2, 3, 6, 12, 24 hours were obtained from 10 stations installed in the pilot areas. Similarly, extreme rainfalls of the duration of 24 hours for the 21 stations were obtained from the Department of Hydrology and Meteorology (DHM).

The hourly series for each network station of the same period were extracted and are correlated with 24 hours, 48 hours, and 72 hours of rainfall. The correlation coefficients are determined. A probabilistic method was applied to calculate the threshold with limited data on rainfall intensity and accumulated precipitation. Warning levels were defined and the corresponding rainfall threshold values were determined by the probability lines.

3. Literature review

The interplay between topography and Indian summer monsoon circulation profoundly controls precipitation distribution, sediment transport, and river discharge along the southern Himalayan mountain front. In the eastern and central parts of the Himalayas, precipitation shows a strong gradient, with high values at medium elevations and extensive penetration of moisture along the major river valleys in the region. The precipitation in these regions has significantly increased and triggered extensive erosional processes on sparsely vegetated steep hill slopes. The mean rainfall along the low to medium elevations was not significantly greater in magnitude (Bookhagen, Thiede *et al*., 2005). In situations, where slopes are extensively terraced for agriculture, with some terraces being intensely irrigated and others not, relationships between landsliding and rainfall amounts are complex and no simple explanations can be made (Gerrard & Ram, 2000). The seasonal rainfall accumulation and the daily rainfall have the capacity to trigger landslides. An analysis of 3 years of daily sediment load and daily rainfall data in the Annapurna region of Nepal, suggested that, for a given hillslope, regolith thickness determines the seasonal rainfall necessary for failure, whereas slope angle controls the daily rainfall required for failure (Gabet *et al*., 2004).

Assessing the risks of landslides requires the historical and current causes that trigger landslides. When studying rainfall and its impact on landslides, it is better to have a history of the area of landslides, when and how it occurred in the particular place and whether it is caused by a high intensity of rainfall or continuous rainy days with heavy rainfall or land erosion from a number of years due to forest clearing or improper land use, or unplanned heavy construction, or unplanned mining. Although it is somewhat baffling whether climate change has any impact on extreme rainfall events in the entire Himalayan region, especially, in recent years, the period 2001-2007 (Nandargi *et al*., 2011), it will too early to ignore the impact of climate change on landslide occurrences. Furthermore, climate change has a direct influence on the frequency and intensity changes in precipitation (Fischer *et al*., 2015), thus increasing the number of potential future landslides (Trenberth, 2011). Landslides pose serious threats to lives and livelihoods, cause hundreds of deaths each year, disrupt local agricultural productivity, damage infrastructure, and cause serious economic disruption both locally and nationally. Therefore, it is necessary to understand how precipitation patterns change with time and the nature of their direct relationship with natural hazards such as landslides.

He *et al*. (2020) conducted a study on landslide events that occurred between 1998 and 2017 in China. The slope of thresholds in events with long durations is higher than that with short durations for thresholds below the quantile level of 50%. They have assumed the causes are due to different mechanisms of landslides triggered by long-term rainfall and short-term rainfall. Evaporation and previous rainfall become more important for landslides triggered by long-duration rainfall events. In addition, the rainfall thresholds in the non-rainy season are generally lower than those in the rainy season. Their research was aimed to establish rainfall thresholds for its application in landside early warning systems. In addition to triggering factors, the geological environment is also important, which decides the susceptibility to landslides in a specific region. Thus, combining multiple rainfall thresholds with the landslide susceptibility map and using the Realtime rainfall the forecasted rainfall from ensemble numerical weather prediction models, the LEFS will be established to reduce and mitigate property damage caused by landslide disasters. (He *et al*., 2020).

Far western Nepal receives 70-80% of its annual precipitation during the monsoon season, between June to September (Nayava, 1974), increasing the occurrence of landslides during this period of the year (Government of Nepal 2019; World Bank 2021). In a global data set of landslides, Nepal contributes 10% of all rainfall-induced landslide events and 93% of all those triggered by seasonal monsoons (Froude *et al*., 2018).

Variations in rainfall patterns due to climate change affect the flux boundary conditions on the surface of the ground. A possible disastrous consequence of this change is the occurrence of rainfall-induced slope failures (Ayron *et al*., 2015). Exposure to the physiographic characters like elevation of the mountains, windward and leeward orientation of mountains, steepness or the slope, distance from the coast, vegetation, and local waterbodies greatly influence the atmospheric circulation and precipitation

TABLE 4

Rainfall type and intensity

Type	Intensity
Heavy rain	Greater than 7.5 mm per hr.
Moderate rain	2.5 mm/hr. to 7.5 mm per hr.
Light rain	Trace to 2.5 mm/hr.
Trace	0.02 to 0.2 mm per hr. (WMO-No. 8, 7th edition)

patterns. The orographic effect also plays a vital role in generating precipitation intensities. Orography affects convection and convergent action, and precipitation intensity depends on the stability of the air mass involved. As a result of mountain topography, rainfall may become more intense, making the weather more extreme, possibly causing severe flooding and drought at different times (Kristo *et al*., 2017). The intensity of the rain is the ratio of the total amount of rain to the duration of the rainfall period. It is expressed in depth units per unit time, usually as millimeters per hour (mm/h). On the basis of intensity, rainfall is classified (Subramanya, 1991) as in Table 4.

Spreen (1947) correlated mean seasonal winter precipitation with 5 factors like elevation, slope, rise, orientation, and exposure for western Colorado found that these five parameters together accounted for 85% of precipitation variation, while elevation alone accounted for about 30% of variation (Singh *et al*., 1995). Similar results were also found by Bums (Bums, 1953) in the small-scale topographical effects in the San Gabriel Mountains in California.

A study on the distribution of seasonal and annual rainfall over a part of Himalayan region was carried out by Singh *et al*. (1995). The role of orography in the middle Himalayas was very pronounced for both rainfall and snowfall compared to other Himalayan ranges. Rainfall increased linearly with elevation in the outer Himalayas on both the windward and leeward sides, except during the monsoon season. In the monsoon season, rainfall increased with elevation up to a certain height and then started to decrease. Rainfall followed a similar distribution with elevation on both windward and leeward sides, *i.e*., first it increased with elevation and then started decreasing. The rainfall distribution fitted well with second-order polynomials. The region of maximum rainfall on the windward and leeward sides was found to be between 1600 and 2200 m. Rainfall decreases exponentially with elevation in the higher Himalayas and becomes negligible at elevations above 4,000 m. Lower rainfall intensity and a lesser number of rainy days are found in the higher Himalayas. An increase in rainfall intensities with elevation is found to be responsible for higher amounts of rainfall on the windward side of the middle Himalayas, while a greater number of rainy days at higher elevations on the leeward side contributed to higher rainfall in the middle Himalayas (Singh *et al*., 1995).

Temporal variations in rainfall over Nepal from 1971 to 2000 m have also been studied (Nayava, 2004). Assessments on rainfall characteristics in the Bajedi landslide in the far-western Nepal also indicated that the rainfall intensity increased by 40-60% over an increase in elevation from 1 to 2 km (Nayava, *et al*., 2022). Rainfall intensities recorded on the leeward side of a slope are lower than the equivalent totals on the windward side. In a certain topography, there is a positive correlation between elevation and the number of days in which rainfall was observed, indicating strong orographic precipitation trends during westerly disturbances. The Himalayan ranges, being the barrier to the monsoon, favor heavy to very heavy rainfall in the foothills and the adjoining plains of India to its south (Dhar *et al*., 1975, 1976). Heavy rainfall is not observed to occur in a continuous period in the plain regions of India, but there can be sudden falls of heavy rain of short (3 to 4 hours) to long (10 to 14 hours) duration. (Nandargi *et al*., 2011).

In the Nepal Himalayas, maximum rainfall has occurred near the outer Himalayas, that is, foothills, and a second maximum has been found near the middle Himalayas at about 2400 mamsl. Then after, rainfall decreases sharply as the elevation increases to higher elevations until the Great Himalayan Range (Dhar *et al*., 1976. Dhar *et al*., 1981). Throughout the Himalayan region, stations at higher elevations have recorded fewer extreme one day rainfalls of 100 to 200 mm, while low-level stations with altitudes <1500 meters have recorded more extreme one day rainfall in the range 700 to 900 mm during the three monsoon months of July, August and September. One day extreme rainfall events have also occurred in the El Niño years and follow the trend of the frequency of active monsoon disturbances which also leads to a decrease in extreme rainfall events (Nandargi *et al*., 2006).

A study conducted in different geomorphological units and geographical regions of Chile has indicated that the precipitation concentration displays an exponential curve where 30% of the rainiest days were concentrated in only 10% of days with precipitation, proving high irregularity (Lozano-Parra *et al*., 2022). Annual precipitation events of 10 and 20 mm are quite common during the monsoon season in many parts of Nepal (Chalise *et al*., 1996).

The high intensity precipitation and the annual precipitation trends showed a significant increase in the middle mountains and hills of the West and the region of the central high mountains of Nepal. A significant positive trend is observed in the number of consecutive dry days but a significant negative trend is observed in the number of wet (rainy) days across Nepal, implying the prolongation of the dry spell throughout the country. Overall, the intensification of different precipitation indices in various parts of the country indicated region-specific risks of floods, landslides and droughts (Karki, *et al*., 2017).

Compared to other events, a large number of deaths occurred due to landslides and debris torrents. The swollen River due to debris torrents also are threat to the settlements on the river bank in the hilly region. A settlement named Olena village in far western Nepal was an exemplary event threatened by the swollen Budhiganga River due to which 87 people of 12 families were displaced on August 13, 2020 (Singh, 2020). A study on trends in landslide occurrence in Nepal by Petley *et al*. (2020) indicated that landslide-induced deaths are being concentrated in the hill districts of the Middle Himalayas of Nepal. Interestingly, the relationship shows that when the summer SW Asian monsoon is intense, the number of fatalities is low and *vice-versa* (Petley, *et al*., 2020).

Numerous scientific evidence have indicated the increasing impact of climate change. The likely disastrous consequence of variations in rainfall patterns is the occurrence of rainfall-induced slope failures. A similar study was conducted on historical rainfall in Singapore, and using the derived trends, projected rainfall intensities in 2050 and 2100, seepage and slope stability analyzes were performed on a typical residual soil slope. Stability analyzes showed a significant decrease in factor of safety from 2003 to 2050 due to an increase in rainfall intensity, suggesting that climate change could have existed beyond 2009 with possibly detrimental effects on slope stability (Kristo *et al*., 2017). Short-duration rainfall is critical for small catchments where there is always a shortage of short-duration rainfall data. In such a case, long-term data from rainfall stations in the same area can be used to develop a very good, statistically acceptable (R^2>0.90) relation between short-duration rainfall and daily rainfall data (Mamun, Salleh & Noor, 2018). In some cases, an empirical technique has been applied to rainfall data in order to determine the intensity-duration-frequency characteristics of rainfall and the underlying distribution (Dar *et al*., 2016).

A regional approach to rainfall frequency analysis with regional information from surrounding stations provides limited information to the area having relatively short periods of record (Smithers *et al*., 2000). Mamun *et al*. (2018) used statistical analysis and logarithmic graph fitting techniques and found an excellent correlation between short-duration rainfall and daily rainfall values for 96 automatic and 46 manual stations in the Klang Valley in Malaysia. The 15, 30 and 45 min of short-duration rainfall were observed to be 32.4%, 47.1% and 57.4% of the daily rainfall amount, respectively. The amount of rainfall during 1h, 2h and 3h storm events contributes 64.9%, 76.5% and 80.9% of the daily rainfall.

Estimation of rainfall intensities and depth duration is essential for various purposes related to water resources and water-induced disaster risk management. The rainfall intensity in mm/hr. for each time period is calculated and are ranked by sorting heaviest to lightest for each time period. The lightest intensity will receive the highest rank, and the highest intensity will receive the lowest rank. The heaviest rains have a lower probability of occurring. The return period is calculated using the Weibull formula. The rainfall intensity versus return period for each rainfall time period is plotted. A data matrix of rainfall intensities for 2-yr, 5-yr 10-yr and 20-year return periods and 15 min, 30 min,1, 2, 3, 6, 12-, 24-, 48- and 72-hour time periods is prepared. Plot a 5-year, 10-year, and 25-year IDF curve (using data points). The IDF curves can be drawn using the mathematical formula established as given equation 1.

The IDF curves are a function of the rainfall intensity (I). IDF equations are empirical equations as expressed below.

$$I = \frac{CT^m}{Td^e} \tag{1}$$

where I is the rainfall intensity in mm/hr.; T is the return period in years and T_d is the duration of rainfall in days. C, m and e are known as the regional constants. (He *et al*., 2020).

Two empirical equations (Talbot and Sherman) are given below (Maxfield, 2009; Nhat *et al*., 2006).

Talbot equation

$$I = \frac{a}{(d+b)} \tag{2}$$

Sherman equation (Sherman, 1931)

$$I = \frac{a}{(d+b)^e} \tag{3}$$

where I is the rainfall intensity (mm/hour); d is the duration (minutes); a, b and e are the constant parameters related to the metrological conditions.

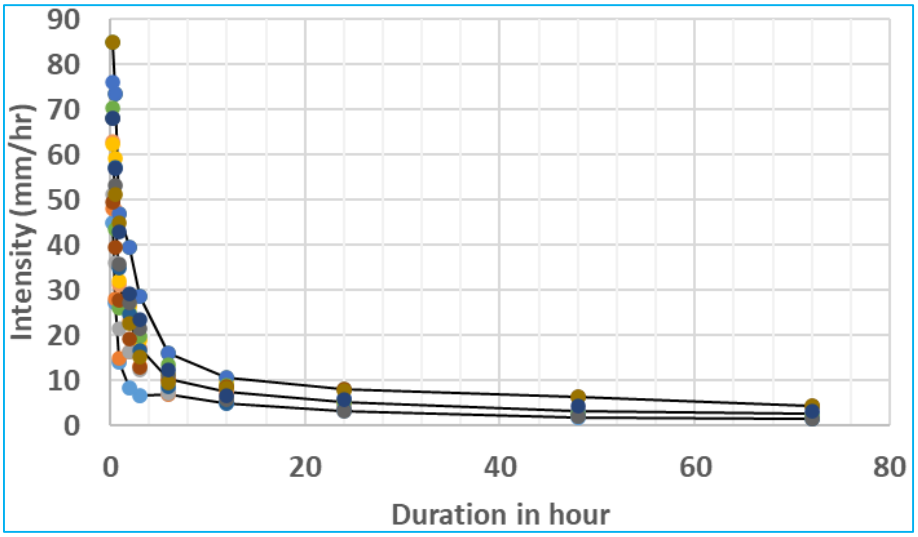

Fig. 6. Rainfall intensities at different durations corresponding to maximum, minimum and average depths

TABLE 5

Rainfall intensities corresponding to maximum, minimum, and average depths

Duration/ mm/hr.	15 min	30 min	1 hour	2 hour	3 hour	6 hour	12 hour	24 hours	48 hours	72 hours
Maximum Intensity	84.8	73.6	47.0	39.5	28.7	16.0	10.6	8.0	6.4	4.4
Minimum intensity	44.8	27.2	14.0	8.5	6.7	7.0	4.8	3.1	1.9	1.5
Average intensity	62.8	47.8	31.1	23.2	17.2	10.5	7.4	5.2	3.3	2.5

The rainfall intensities and rainfall depth also depend on the storm coverage, how large an area is covered, and how long it lasts. Rainfall depth-area relation from data of the July flood of 1993 flood event was analyzed (Bhusal, 1994). It is being difficult to demark the coverage of an area of active storm giving intense rainfall, isohyet maps were prepared and the area between isohyet lines were measured. Rainfall depth over 24 hours and 48 hours was determined and correlated with area. Based on observed rainfall data during 1993 storms, the following equation (4) was established to estimate the extreme rainfall depths over the south central region, Nepal (Marahatta *et al.*, 2009).

$$P = 1.5P_0 * \exp\left\{\frac{-\ln(A)}{6}\right\} \quad (4)$$

where, A is catchment area (km^2), ln (A) is the natural logarithm of area A, P is the rainfall depth of desired duration (mm) in 24- or 48-hours duration, and P_0 is the maximum observed rainfall (mm) of (24-h or 48-h) at the center location of the storm. In 1993, the observed P_{24} and P_{48} was 540 mm and 600 mm respectively in south-central Nepal.

Indian Meteorological Department (IMD) targets estimating rainfall intensity of any return period with the least amount of effort (Chowdhury *et al.*, 2007). The equation (5) is as follows:

$$Pt = P24\left(\frac{t}{24}\right)^{\left(\frac{1}{3}\right)} \quad (5)$$

Where Pt is the required rainfall depth in mm at t-h duration, $P24$ is the daily rainfall in mm and t is the duration of rainfall, for which the rainfall depth is required in hr.

4. Results and discussions

From the data series in the tables above, the maximum, the minimum, and the average values are computed. Rainfall intensities corresponding to maximum, minimum, and average depths are computed and given in Table 5 and shown in Fig. 6.

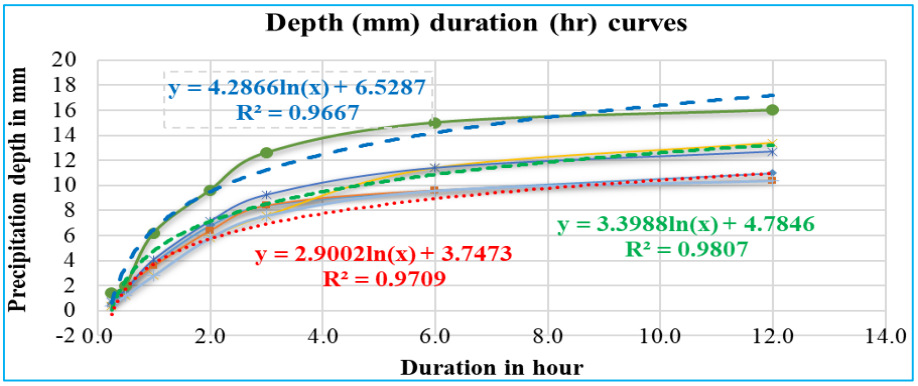

Fig. 7. The best-fit depth-duration curves on upper, average and lower rainfall depths

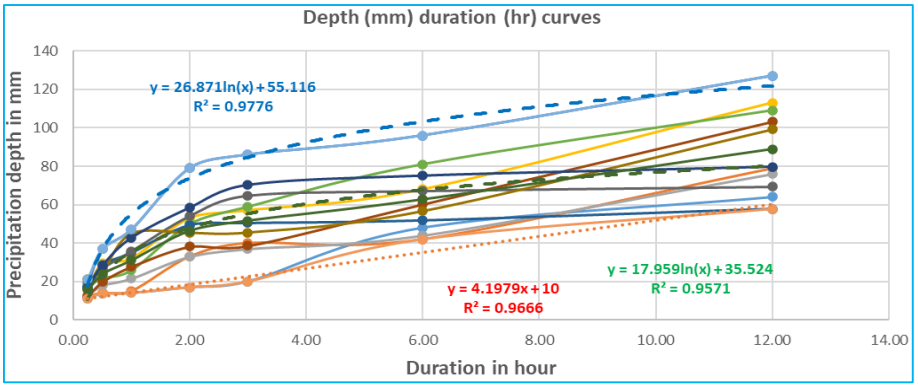

Fig. 8. Depth-duration curves on 15 min to 12 hr. durations

TABLE 6

Rainfall depths at different durations (up to 12-hr) on observation data

Location	Ele(m)	15 min	30 min	1hour	2hours	3hours	6 hours	12 hours
24 hour rainfall recorded on 12 July, 2019								
Asha Hotel	1020	0.6	1.6	3.8	6.8	8.4	9.6	11
Olena	1116	0.4	1.2	2.8	5.8	7.6	11.4	13.4
Thuma Sec. School	1447	1.4	2	3.6	6.4	8.4	9.6	10.4
Near lake	2040	0.6	2	6.2	9.6	12.6	15	16

4.1. *Trend of rainfall depths-durations*

The one day rainfall of the following four locations was less than 20 mm on 12 July, 2019. The duration of the storm lasted for 12 hours only. Rainfall depths with duration are given in Table 6. The best fit curves followed logarithmic tend lines, which are shown in Fig. 7.

The best-fit trendlines for the observed rainfall depths of different durations (Table 2) indicated that the duration of the rainfall depth in the pilot areas followed the logarithmic trend (Fig. 8) for the maximum and average rainfall depths of 15 minutes to 12 hours. But, for rainfall depths of 15 minutes to 72 hours, the trend line (Fig. 9) followed the power relations to maximum rainfalls (R^2 = 97), minimum rainfall (R^2 = 98) and average rainfalls (R^2 = 97),

The relationship between intensity and duration is established by the trend line fitting (regression) by inbuilt

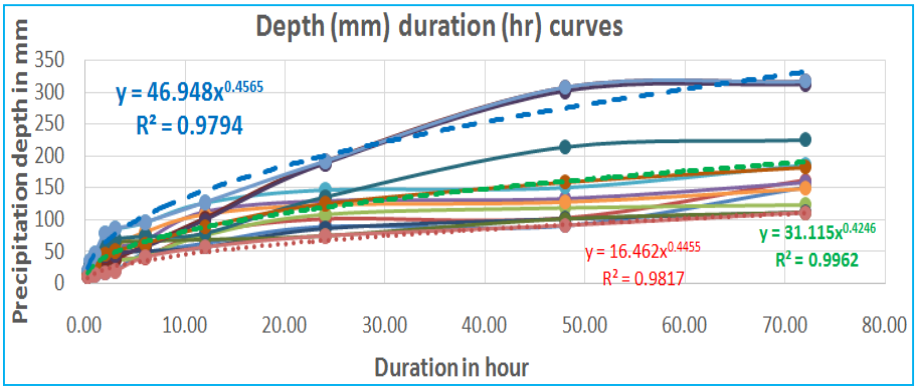

Fig. 9. Depth-duration curves on 15 min to 72-hr durations

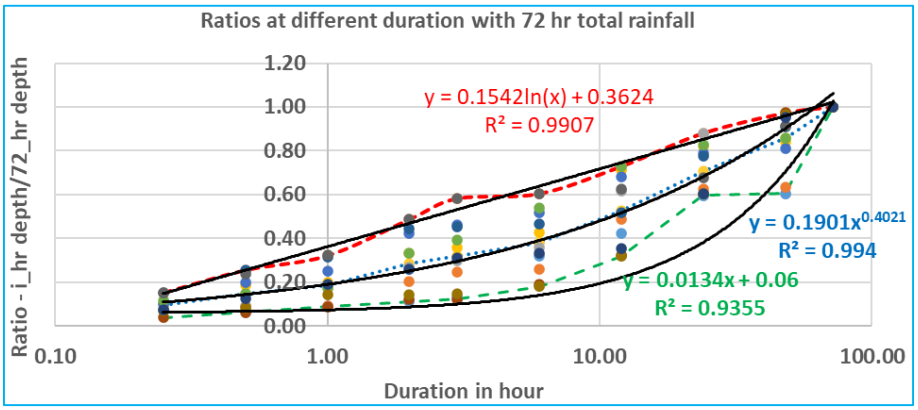

Fig. 10. Rainfall depth ratio-duration curves for durations up to 72 hr rainfall

program in Microsoft Excel. The resulting formulae for maximum, minimum and average intensities are given below.

$$I\_\max = 46.948\, d^{(-)0.543} \quad \left(R^2 = 0.9673\right) \tag{6}$$

$$I\_avg = 31.115\, d^{(-)0.575} \quad \left(R^2 = 0.9919\right) \tag{7}$$

$$I\_\min = 16.462\, d^{(0.555)} \quad \left(R^2 = 0.9667\right) \tag{8}$$

On the basis of the above data, a generalized formula is derived as follows.

$$I = \frac{\mathrm{K}}{\sqrt{d}} \tag{9}$$

I is the intensity of the rain (mm/h), d is the duration in hour, and K is a constant. The generalized value of K is 16 for minimum intensity, 32 for mean intensity and 48 for maximum intensity.

4.2. *Threshold rainfall depths*

To understand and get a generalized pattern, regression between rainfall depth ratio and duration is carried out to understand how rainfall depth (intensities) varied with passes of the time after any storm starts down pouring. Rainfall depth ratio on observed data of each location at each duration (15-m to 72-hr) are determined, dividing by 72-hours, 48-hours, 24-hours and 12-hours and so on. Rainfall depth ratios are correlated with durations. Correlations are satisfactory, giving correlation coefficients ranging from 0.93 to 0.99. Only, rainfall depth ratios with 72-hour duration to the maximum, the minimum, and the average values (listed at the bottom of the Table 2) are given in Table 7. The Fig. 10 shows corresponding best fitted curves. The use of such correlation is helpful to assess the rainfall depths of shorter durations as required. This approach is appropriate

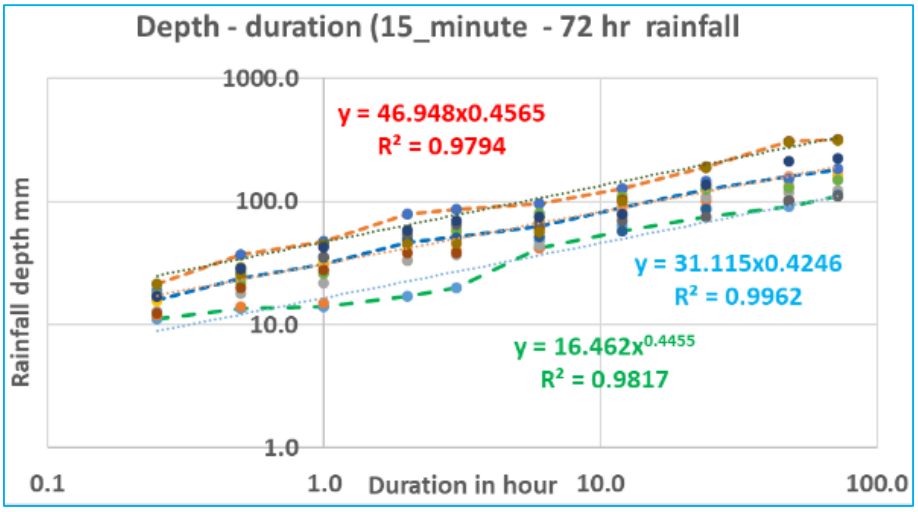

Fig. 11. Depth duration curve (15-min to 72-hr duration)

TABLE 7

Rainfall depth ratios with 72- hour rainfall

Durations/Ratios	15 min	30 min	1 hour	2 hours	3 hours	6 hours	12 hours	24 hours	48 hours	72 hours
Average rainfall/72- h rain	0.10	0.15	0.19	0.28	0.32	0.38	0.53	0.71	0.86	1.00
Maximum rainfall/72- h rain	0.15	0.26	0.32	0.49	0.58	0.60	0.73	0.88	0.97	1.00
Minimum rainfall/72- h rain	0.04	0.06	0.09	0.11	0.12	0.18	0.32	0.60	0.60	1.00

to Nepal as there are several locations where only 24 hr. total rainfall is recorded.

4.2. *Threshold rainfall depths*

The intensity and duration of rainfall in the rainy season are the main factors that cause water-induced landslides. A certain rainfall depth that does not cause any landslides at one location nor at one watershed morphology and topography may be the cause of landslides at another location. The same rainfall depth that cannot cause a landslide in one season may be the cause of a landslide in another season. Therefore, determining threshold rainfall related to landslide is to find the best correlation with multiple parameters, such as in the USLE (universal soil loss equation) (Wischmeier & Smith, 1978). However, this paper has attempted to find some thresholds based on results of rainfall depth duration analysis. The following 24-hour rainfall depths for the 2019 monsoon (rainy season) are screened from Table 3, which had caused landslides in the region.

Screened data are:

(*i*) First day (24 hr) depth lying between 27.4 mm and 126.2 mm.

(*ii*) Second day (24 hr.) depth lying between 20.2 mm and 81.3 mm, and cumulative depth lying between 38.6 mm and 89.3 mm, respectively.

(*iii*) 3rd day (24 hr.) depth lying between 27.5 mm and 111.8 mm, and cumulative depth lying between 51.1 mm and 117 mm, respectively.

(*iv*) Fourth day (24 hr.) depth lying between 19.3 mm and 43.4 mm and cumulative depth lying between 58.0 mm and 68.8 mm, respectively.

(*v*) Fifth day (24 hr.) depth lying between 19.4 mm and 22.7 mm and cumulative depth lying between 73.7 mm and 59.8 mm, respectively.

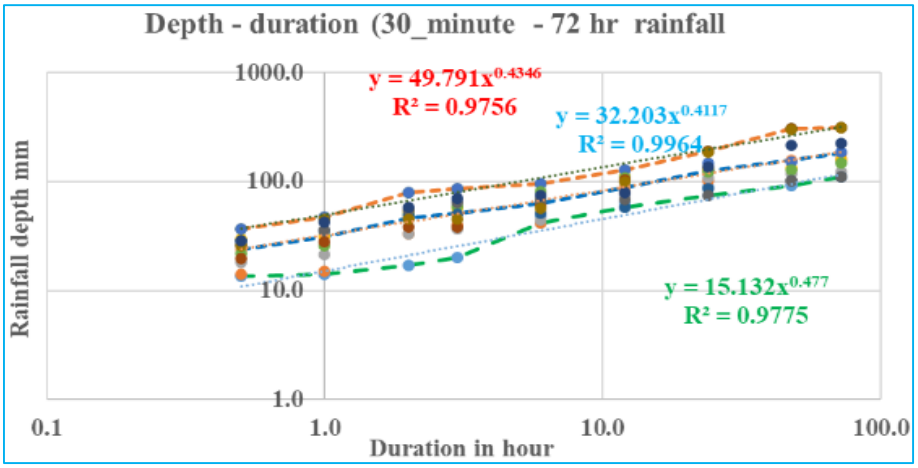

Fig. 12. Depth duration curve (30 min to 72 hr. duration)

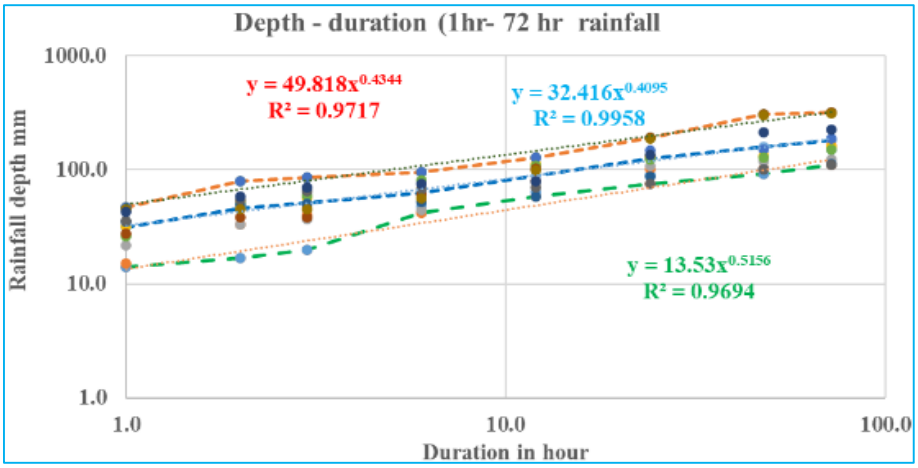

Fig. 13. Depth duration curve (1-hr to 72 hr duration)

In Nepal, rainfall intensity reaches maximum in a short period of time and decreases exponentially. The rainfall data for the region that are summarized in Table 3 are 24 hr. Daily totals. Therefore, to establish the general trend, the maximum, minimum, and average rainfall depths and corresponding duration in observed data (listed in Table 2) are correlated with the durations of 15 minutes, 30 minutes, 1 hour and 2 hours. Figs. 11, 12, 13&14 give the respective relationships of graphical presentation in logarithmic scales.

4.4. *Selection of threshold*

The depth duration curve derived from average values is considered as a threshold curve, and the curve corresponding to the maximum values is considered to indicate a substantial risk alerting line. Similarly, the curve corresponding to the minimum values is considered a minimal risk line. Table 8 contains the corresponding rainfall depths from the best fit relationships (Figs. 9&11, Equation no. 6, 7 and 8 as given).

For flood forecasting purposes, the Department of Hydrology and Meteorology has considered the threshold values of 60, 80, 100 and 120 mm of rainfall over 1, 2, 3, and 24 hours, respectively (DHM, 2019) (Nayava, *et al*., 2022). The data derived in this paper are comparable to the DHM values.

4.5. *Practical application*

For the prediction and issuing warning for landslides, the relationships between rainfall depth ratio to shorter duration like 15 minutes, 30 minutes, one hour *etc*. are desirable. Therefore, a regression analysis was carried out on ratios of rainfall depth to different durations of

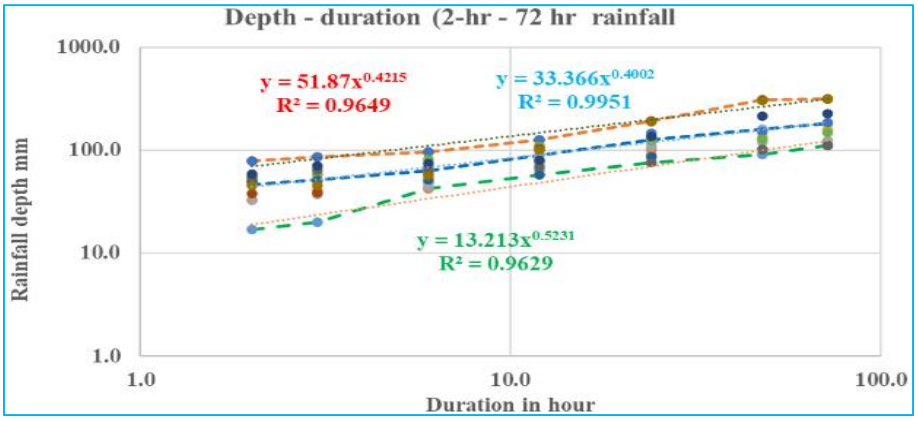

Fig. 14. Depth duration curve (2-hr to 72-hr duration)

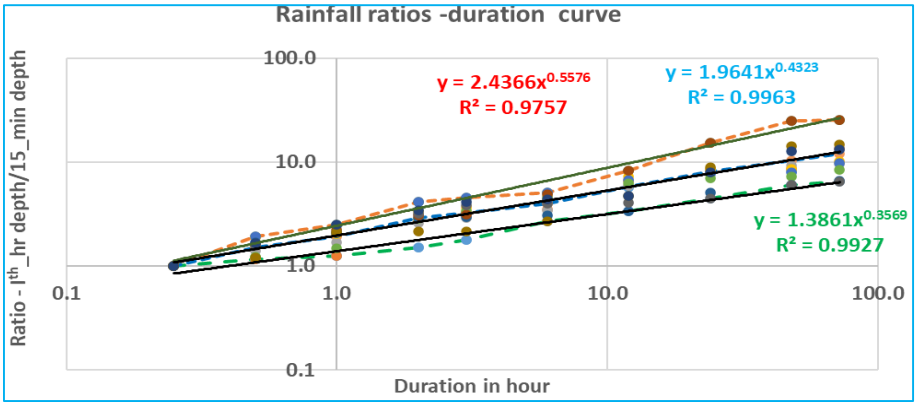

Fig. 15. Rainfall depth ratio-duration curves for durations 15-min to 72-hr

TABLE 8

Threshold rainfalls

Rainfall depth (mm)										
Duration	15-m	30 m	1-h	2-h	3-h	6-h	12-h	24-h	48-h	72-h
High rainfall	24.9	35.5	48.9	67.1	79.3	107.6	146.0	198.2	269	321.8
Threshold	17.3	23.7	31.9	42.9	50.6	67.3	89.6	119.2	158.6	187.5
Low rainfall	8.9	11.5	15.0	20.5	25.0	35.1	49.3	69.2	97.3	118.8

TABLE 9

Multiplying coefficients to 15-min duration rainfall rain (observed) for calculating rainfall at rainfall depth at different durations

Multiplying coefficients to 15 min rainfall										
Duration	15-m	30 m	1-h	2-h	3-h	6-h	12-h	24-h	48-h	72-h
High rainfall	1.1	1.7	2.4	3.6	4.5	6.6	9.7	14.3	21.1	26.5
Threshold	1.0	1.4	1.9	2.6	3.1	4.2	5.7	7.7	10.4	12.4
Low rainfall	0.8	1.1	1.4	1.8	2.1	2.6	3.4	4.3	5.5	6.4

15 minutes, 30 minutes, 1 hour and 2 hours. In all, the correlation coefficients ranged from 97% to 99%, showing a good correlation. The power relation is found to be highly correlated. Corresponding best-fit curves relating to maximum, average and minimum are shown in Fig. 15. The estimated values using established formulas (Equations 10, 11, 12) are tabulated in Table 9. These values are the multiplying coefficient to predict the likely rainfall at different durations from observed 15-minute rain fall. The observed rainfall for 15 minutes duration is multiplied by factors given in Table 9 (See note given below the table) and a table similar to the Table 8 is generated which indicates whether rainfall trends is on risk side or not. Similarly, tables with multiplying factors for desired durations like 30 min 1 hr. *etc.* are to be derived and used for landslide awareness.

$$R_{dr\_\max} = 2.4366\, d^{0.5576} \quad \left(R^2 = 0.9757\right) \tag{10}$$

$$R_{dr\_avg} = 1.9741\, d^{0.4323} \quad \left(R^2 = 0.9963\right) \tag{11}$$

$$R_{dr\_\min} = 1.3861\, d^{0.3569} \quad \left(R^2 = 0.9927\right) \tag{12}$$

5. Conclusions

The maximum intensity of rain of 84 mm / hour and 74 mm / hour were recorded in the Sunkunda pilot area at a duration of 15 min and a duration of 30 min, respectively. These values are higher than the maximum intensity of rainfall of 70 mm/hr. observed in central South Nepal during the 1993 catastrophic storm. The 1-hour and 24-hour total during the 1993 storm were 70 mm and 540 mm in the southern central Nepal, while these values are only 45 mm and 188 mm respectively in the Sunkunda area in 2019.

The landslide that caused the rain varied widely. Landslides are recorded for 24-hour rainfall of 27.4 to 126.2 mm in the pilot region in 2019 but are not deadly like the catastrophic events of 1993. The analysis supported the fact that the antecedent precipitation index (API) has a great effect on maturing (wetting) the land to slide even with lower rainfall depths.

The analysis of the observed rainfalls for 2019 resulted in a generalized trend of the relationship between intensity and duration. The trend lines of rainfall depths-durations on observed data showed excellent fitting. Therefore, the trend line of the average depth of rainfall is considered as the threshold rainfall line, a tool for determining the probability of land slip probability.

The threshold rainfall depth determined in the preceding chapter is based on rainfall data observed during 2019 and 2021 for the specific location (pilot area) of the EVO landslide research study. Although the analysis is performed from one-year data, it requires verification with more-year data. However, in the region where continuous recording of rainfall by automatic recorders is not available, the coefficients determined from observed data are to be considered for threshold rainfalls for the warning system.

Acknowledgements

Data for this paper have come from the research consortium funded by the UK Natural Environment Research Council (NERC) and DFID as project NE/P000452/1 (Landslide EVO) under the SHEAR program, and from the Department of Hydrology and Meteorology (DHM), Government of Nepal. The authors express gratitude to DHM and Landslide EVO, Imperial College.

Disclaimer : The contents and views expressed in this research paper/article are the views of the authors and do not necessarily reflect the views of the organizations they belong to.

References

Bookhagen, B., Thiede, B. and Strecker, M., 2005, "Abnormal monsoon years and their control on erosion and sediment flux in the high, arid northwest Himalaya," *Earth and Planetary Science Letters*, **231**, 1-2, 131-146.

Bums, J. I., 1953, "Small-scale topographic effects on precipitation distribution in San Dimas Experimental forest", *Trans. Amer. Geophys.Un.*, **34**, 761-768. Retrieved from http://117.252.14. 242/Gangakosh/Publications/NIH_Publications/Full%20papers/ pratap12.pdf.

Chalise, S. R, Shrestha, M. L, Thapa, K. B, Shrestha, B. R. and Bajracharya, B., 1996, "Climatic and Hydrological Atlas of Nepal. Kathmandu," Nepal: ICIMOD.

Chowdhury, R., Alam, Md. J. B., Das, P. and Alam, Md. A., 2007, "Short duration rainfall estimation of Sylhet IMD and USWB method," *Journal of Indian Waterworks Assoc*, **39**, 4, 285-292.

Cieslik, K., Shakya, P., Uprety, M., Dewulf, A., Russell, C., Clark, J., Dhakal, A., 2019, "Building Resilience to Chronic Landslide Hazard Through Citizen Science", *Front. Earth Sci., 7*, 278. doi : https://doi.org/10.3389/feart.2019.00278.

Dahal, R. K., 2012, "Rainfall-induced landslides in Nepal", *International Journal of Erosion Control Engineering*, **5**, 1, 1-8. doi : 10.13101/ijece.5.1

Dar, A. Q., Maqbool, H. and Raazia, S., 2016, "An empirical formula to estimate rainfall intensity in Kupwara region of Kashmir valley, J&K, India," MATEC Web of Conferences. doi : 10.1051/ 57, 03010, matec 57 conf/2016 0 ICAET 2016 - 301.

Dhar, O. N. and Bhattacharya, B., 1976, "Variation of rainfall with elevation in the Himalayas-a pilot study," *Indian Journal of*

Power and River Valley Development, **26**, 6, 179-186. Retrieved from Google Scholar.

Dhar, O. N. and Rakhecha, P. R., 1981, "The effect of elevation on monsoon rainfall distribution in the Central Himalayas," *International Symposium on Monsoon Dynamics*, 253-260. Cambridge: Cambridge University Press. Retrieved from : Google Scholar.

Dhar, O. N., Kulkarni, A. K. and Sangam, R. B., 1975, "Study of extreme point rainfall over flash flood prone regions of the Himalayan foot hills of north India. *Hydrological Sciences Bulletin*, 20, 61-67. Retrieved from https://www.tropmet.res.in/~lip/Publication/p-1975.html

Dhital, M. R., 2022, "Juxtaposition of Greater and Lesser Himalayan nappes in west Nepal: implications for delineating Main Central Thrust", *Himalayan Geology,* **43**, 18, 231-240.

Fischer, E. M. and Knutti, R., 2015, "Anthropogenic contribution to global occurrence of heavy-precipitation and high-temperature extremes", *Nature Climate Change*, **5**, 6, 560-564.

Froude, M. J. and Petley, D. N., 2018, "Global fatal landslide occurrence from 2004 to 2016", *Natural Hazards and Earth System Sciences*, **8**, 8, 8, 2161-2181.

Gabet, E. J., Burbank, D. W., Putkonen, J. K., Pratt-Sitaula, B. A. and Ojha, T., 2004, "Rainfall thresholds for landsliding in the Himalayas of Nepal", *Geomorphology*, **63**, 131-143. doi : 0.1016/j.geomorph.2004.03.011.

Gerrard, A. and Ram, G., 2000, "Relationships between rainfall and landsliding in the Middle Hills Nepal", *Norsk Geografisk Tidsskrift*, **54**, 74-81.

Government of Nepal, 2019, "Nepal Disaster Report 2019*",* Kathmandu: Ministry of Home Affairs. Retrieved from http://drrportal.gov. np/uploads/document/1594.pdf

He, S., Wang, J. and Liu, S., 2020, "Rainfall Event–Duration Thresholds for Landslide", *Water*, **12**, 494. doi : 10.3390/w12020494.

Karki, R., Hasson, S. U., Schickhoff, U., Scholten, T. and Böhner, J., 2017, "Rising Precipitation Extremes across Nepal," (C. Anagnostopoulo, Ed.) *Climate*, **5**, 4, 1-25. doi : 10.3390/ cli5010004.

Kristo, C., Rahardjo, H. and Satyanaga, A., 2017, "Effect of variations in rainfall intensity on slope stability in Singapore", *International Soil and Water Conservation Research*. Retrieved from www.elsevier.com/locate/iswcr.

Mamun, A. A., Salleh, M. N. and Noor, H. M., 2018, "Estimation of short duration rainfall intensity from daily rainfall values in Klang Valley, Malaysia," *Applied Water Science*, **8**, 203. doi : https://doi.org/10.1007/s13201-018-0854-z.

Marahatta, S. and Bhusal, J. K., 2009, "Relating Hydrological Extremes with Area -A Case on Extreme Floods in South Central Nepal," *Journal of Hydrology and Meteorology*, **6**, 1.

Maxfield, B., 2009, "Development of Intensity Duration Frequency (IDF) Curves", In Essential Mathcad for Engineering, Science, and Math. Academic Press. doi : https://doi.org/10.1016/B978-0-12-374783-9.00011-4.

MoSTE., 2014, Nepal Second National Communication to United Nations Framework Convention on Kathmandu: MoSTE (2014). Nepal Second National Communication to United Nations Framework Convention on climate change. Retrieved from https://unfccc.int/resource/docs/natc/nplnc2.pdf.

Nandargi, S. S. and Dhar, O., 2006, "Tropical disturbances and Indian monsoon rainfall", *Journal of Applied Hydrology*, **19**, 3, Special issue), 1-7. Retrieved from Google Scholar.

Nandargi, S. and Dhar, O. N., 2011, "Extreme rainfall events over the Himalayas between 1871 and 2007", *Hydrological Sciences Journal*, **56**, 6, 930-945. doi :10.1080/02626667.2011.595373.

Nayava, J. L., 1974, "Heavy monsoon rainfall in Nepal", *Weather,* **29**, 443-450.

Nayava, J. L., 2004, "The temporal variations in rainfall in Nepal since 1971 to 2000", *Journal of Hydrology and Meteorology*, **1**, 1, 24-33.

Nayava, J. L., Bhusal, J. K., Paul, J. D., Buytaert, W., Neupane, B., Gyawali, J. and Poudyal, S., 2022, "Changing precipitation patterns in far-western Nepal in relation to landslides in Bajhang and Bajura districts," *The Geographical Journal of Nepal*, **15**, 23-40. doi : https://doi.org/10.3126/gjn.v15i01.42891.

Nhat, L. M., Tachikawa, Y. and Takara, K., 2006, "Establishment of Intensity-Duration-Frequency Curves for Precipitation in the Monsoon Area of Vietnam," *Annuals of Disaster Prevention Research Institute*, **49B**, 93-103.

Parajuli, B., Khadka, P., Baskota, P., Shakya, P., Pudasaini, W. L., Paul, J. D. and Vij, S., 2020, "An open data and citizen science approach to building resilience to natural hazards in a data-scarce remote mountainous part of Nepal", Sustainability, **12**, 22, doi : 10.3390/su12229448

Paul, J. D., Cieslik, K., Sah, N., Shakya, P., P. B., Paudel, S., and Buytaert, W., 2020, "Applying citizen science for sustainable development, rainfall monitoring in western Nepal", *Frontiers in Water*, **2**, 1-12.

Petley, D. N., Hearn, G. J., Hart, A., Rosser, N. J., Dunning, S. A., Oven, K., and Mitchell, Shrestha, P. M., 2020, "Planned construction of rural roads and earthquake-hit geology blamed for the damages", *The Kathmandu Post*.

Sherman, C., 1931, "Frequency and intensity of excessive rainfall at Boston, Massachusetts," *Transactions, American Society of Civil Engineers*, **95**, 951-960.

Singh, P., 2020, "Bajura's Olena village at risk of landslide, flood" *The Himalayan Times*. Retrieved January 24, 2021, from https://thehimalayantimes.com/nepal/bajuras-olena-village-at-risk-of-landslide-flood/

Singh, P., Ramasastri, K. S. and Kumar, N., 1995, "Topographical Influence on Precipitation Distribution in Different Ranges of Western Himalayas", *Nordic Hydrology*, **26**, 259-284. Retrieved from http://117.252.14.242/Gangakosh/Publications/NIH Publications/Full%20papers/pratap12.pdf.

Spreen, W. C., 1947, "Determination of the effect of topography on precipitation. Trans," *Am. Geophys. Un*., **28**, 285-290. Retrieved from http://117.252.14.242/Gangakosh/Publications/NIH Publications/Full%20papers/pratap12.pdf.

Strauch, M. Ayron, A. MacKenzie, R., P. Giardina, C. and Brand, G. L., 2015, "Climate driven changes to rainfall and streamflow patterns in a model tropical island, hydrological system", *Journal of Hydrology*, **523**, 160-169. doi : https://doi.org/ 10.1016/j.jhydrol.2015.01.045.(http://www.sciencedirect.com/science/article/pii/S0022169415000621).

Subramanya, K., 1991, Egineering Hydrology. Tata McGraw Hill.

Sudmeier-Rieux, K., McAdoo, B. G., Devkota, S., Rajbhandari, P. C., Howell, J. and Sharma, S., 2019, "Invited perspectives: Mountain roads in Nepal at a new crossroads", *Natural Hazards*

and Earth System Sciences, **19**, 655-660. doi : https://doi.org/10.5194/nhess-19-655-2019.

UN. Office for Disaster Risk Reduction, 2020, United Nations Office for Disaster Risk Reduction : 2019 annual report. Geneva : United Nations Office for Disaster Risk Reduction. Retrieved from https://digitallibrary.un.org/record/3895941

Wischmeier, W. and Smith, D., 1978, "Predicting Rainfall Erosion Losses: A Guide to Conservation Planning," Washington, DC. p58 USDA/Science and Education Administration, US. Govt.

World Bank, 2021, *Global landslide hazard map - Rainfall trigger (1980-2018, median).* Retrieved from https://datacatalog.worldbank.org/search/dataset/0037584/Global-landslide-hazard-map.

Bhusal, J. K., 1994, "Hydrological Aspects of July 1993 flood (South Central Nepal", Second National Conference on Science and Technology, June 8-11, Kathmandu, Nepal: Royal Nepal Academy of Science and Technology.

Lozano-Parra, J., Velarde and Aguirre, I., June 2022, "Extreme Precipitation Events in Chile: Latitudinal and Altitudinal Variations," In J. Lozano-Parra, Velarde, and I. Aguirre, Analyzing Sustainability in Peripheral, Ultra-Peripheral, and Low-Density Regions. doi :10.4018/978-1-6684-4548-8.ch006.